18th Int. Symp. "Nanostructures: Physics and Technology"
St Petersburg, Russia, June 21–26, 2010

Nano-optical emission of single colloidal CdSe nanowires

A. M. Mintairov, J. Herzog, M. Kuno and J. L. Merz
University of Notre Dame, Notre Dame, IN 46556 USA

Abstract. We used near-field scanning optical microscopy (NSOM) having spatial resolution ∼100 nm in combination with diffraction-limited micro-photoluminescence (μ-PL) and time-resolved (TR) spectroscopy to study emission properties of single colloidal CdSe nanowires (NWs). Comparison of NSOM and wide-field μ-PL images allows observation of residual chemical and/or water drops attached to a NW, which act as a nano-lens providing efficient coupling of excited and emitted photons. At temperatures $T < 150$ K the emission spectra of a single NW reveal interference structure (period $\sim\lambda/200$) manifesting strong exciton-polariton coupling. Effects of carrier localization in wurtzite (W) and zinc-blende (ZB) sections of NW were observed in temperature dependent spectra. Type-I band alignment of ZB-W heterojunction was revealed from spectral dependence of emission decay.

Introduction

Recently the synthesis and optical properties of colloidal CdSe NWs have attracted considerable attention [1]. Sharp emission lines were observed in low-temperature micro-photoluminescence (μ-PL) spectra of single CdSe NWs [2]. Such lines manifest exciton localization on zero-dimensional potential fluctuations, which was previously studied in detail in epitaxially-grown GaAs/AlGaAs NWs using high-spatial-resolution near-field scanning optical microscopy (NSOM)) [3]. Here we use temperature-dependent NSOM having spatial resolution ∼100 nm in combination with diffraction-limited μ-PL (spatial resolution ∼1 μm) and time-resolved (TR) spectroscopy to study emission properties and exciton localization in colloidal CdSe NWs.

1. Experimental details

CdSe NWs with mean diameters 20 nm and length exceeding 1 μm were synthesized following a recently-developed solid-liquid-solid growth technique [1]. High-resolution transmission electron microscopy measurements have shown that average length of zinc blende (ZB) and wurtzite (W) sections in NW is 3 and 2 nm, respectively, and that ZB(W) lengths range from 1 to 16 nm (1 to 17 nm). Our NSOM setups based on room-temperature Multi-View 1000 NSOM (NANONICS Imaging Ltd) and low-temperature CryoSXM (Oxford Instruments) heads have been described [4,5]. A home-made inverted microscope with an oil-immersion microscope objective ($\times$100, N.A. = 1.2) was used for diffraction limited wide-field (WF) imaging of an area of $\sim 30 \times 50$ μm^2 in conjunction with NSOM imaging and time-resolved spectroscopy as described in [5].

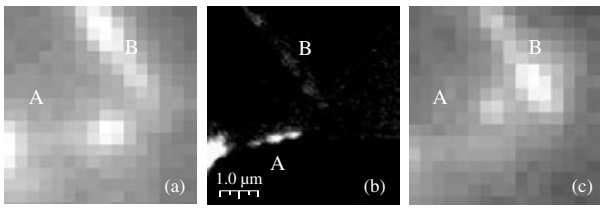

Fig. 1. Comparison of WF (a and c) and NSOM (b) images of two CdSe NWs (A and B) at 300 K. WF images a and c were taken before and after NSOM scans. Image size is $\sim 5 \times 5$ μm^2.

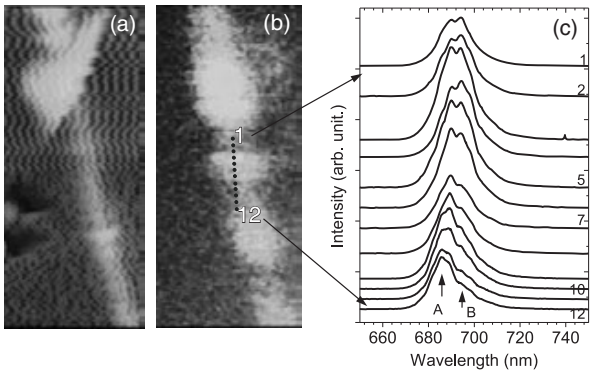

Fig. 2. Topography (a) and NSOM images (b) of CdSe NW (size 40 nm) at 50 K. Spectra (c) were taken along the NW with steps of 50 nm. Image size is 0.8×2 μm^2.

2. Near-field versus wide-field imaging

Fig. 1a–c compares NSOM and WF images of two CdSe NWs (A and B) at room temperature. WF images were taken before and after the NSOM scan. Before the scan (Fig. 1a) the WF image of NW A shows a bright, diffraction-limited circular region at each end. After the NSOM scan (Fig. 1c) the left bright spot disappears and the right one moves up by ∼1 mum. These and other observations [5] show that the NWs have a liquid drop/shell attached, which is "rearranged" by the fiber tip when it touches the wire during scanning. The shell forms a nano-lens, providing near-field coupling of incident and emitted photons, which makes colloidal nanostructures bright in far-field imaging.

3. High-spatial-resolution spectroscopy

Fig. 2a and b show 0.8×2 μm^2 topographic and NSOM images of a CdSe NW taken at 50 K. The NSOM image reveals inhomogeneity of the emission intensity on a length scale of ∼200 nm, similar to that observed at 300 K in Fig. 1b. The 12 spectra taken along the NW with 50 nm steps in Fig. 2c show that intensity variations are accompanied by variations of spectral line shape. Analysis shows that spectra consist of two overlapping bands, having width ∼15 nm, whose relative intensity changes along the NW. The bands are centred at 685(1.810) and 696(1.782) nm(eV) and can be attributed to W and ZB sections of NW as will be shown below. In Fig. 2c the spectra reveal interference structure having a modulation period of 4 nm. We found that the structure appears in NSOM

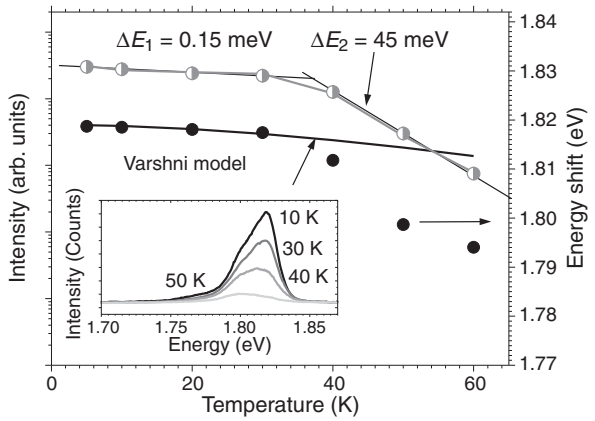

Fig. 3. Intensity and energy shift of CdSe NW PL band (see insert) versus temperature measured by NSOM (half-filled and solid circles, respectively) together with activation model fit (for intensity) and Varshni model band-gap shift (curves). Two straight lines show activation energies 0.15 and 45 meV.

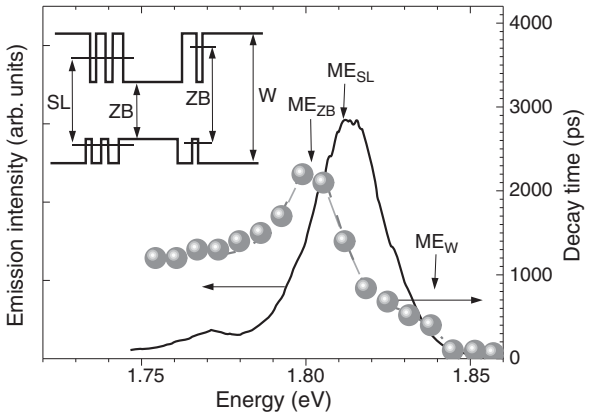

Fig. 4. Energy dispersion of emission decay time $\tau(E)$ (circles) together with time-integrated micro-PL spectra of single CdSe NW at ~10 K (solid curve). Dashed curve is fitting using band-tail model of exciton localization [9]. Insert shows energy structure and W, SL and ZB transitions of along NW.

spectra and TR μ-PL spectra at temperatures below 150 K and can be related to effects of strong exciton-polariton interaction [6].

4. Effects of carrier localization

Fig. 3 shows the temperature dependence of the integrated intensity and the peak position of a NW measured using NSOM spectra at a temperature range $T = 5-60$ K. Insert shows spectra at $T = 10$, 30, 40 and 50 K. A decrease of intensity by one order of magnitude and a red shift of peak position by ~20 meV are observed. The intensity decrease is described by two activation channels having energy $\Delta E_1 = 0.15$ and $\Delta E_2 = 45$ meV, which correspond to mobility edges for SL and W states, respectively (cf. Fig. 4). The shift value of 20 meV observed is much larger then the value of 4 meV expected for thermal expansion effects (Varshni model) [7]. In μ-PL spectra taken over a wider temperature range we observed clear S-type behaviour of the peak position, which manifests the thermal population of band-tail states [8], i.e. existence of strong one dimensional disorder along the NW. Fig. 4 shows typical spectral dependence of emission decay $\tau(E)$ of a CdSe NW together with a time-integrated spectrum. Fig. 4 also shows a cartoon describing zone structure and energy transitions of NW extracted from $\tau(E)$ curve. Similar to Fig. 2 the spectra contain two peaks — a strong one centred at 1.81 and a weak one centred at 1.77 eV. The $\tau(E)$ dependence shows increase of the decay time from 1 to 2 ns in the low energy range of emission spectra (1.75–1.8 eV) followed by a decrease at higher energies (down to $\tau = 65$ ps at 1.86 eV). Near 1.83 eV a plateau at $\tau = 700$ ps is seen. The observed behaviour can be explained assuming type-I band alignment at W-ZB heterojunction. As shown in the band diagram in Fig. 4 three types of transitions are expected for that case, which are (1) W-type transitions, corresponding to extended, tunnel-isolated (<5 nm) wurtzite sections; (2) SL-type transitions, corresponding short-period superlattice sections formed by alternation of a few nm thick, W and ZB sections, and ZB-type transitions, corresponding to isolated zinc blende sections. Since a radiation decay time is inversely proportional to a localization length one can expect a increase (decrease) of the emission decay time versus energy for ZB-type (W- and SL-type) transitions as indeed observed in experiment. We should point out that the decay increase in the low energy range of the emission spectra rule out the type-II band alignment of ZB-W heterojunction. The experimental $\tau(E)$ curve we fitted (see Fig. 4) using band-tail model of exciton localization [9] and accounting for contributions of the three W, SL and ZB transitions. The individual contribution was expressed as

$$\tau(E) = \frac{\tau_{\text{rad}}}{1 + \exp\left[\alpha(E - E_0)\right]}, \qquad (1)$$

where τ_{rad} is the radiation life-time in the strong localization regime and E_0 is a mobility edge (ME). The following values were extracted from fitting: 600 ps for $\tau_{\text{rad W}}$, 2100 ps for $\tau_{\text{rad ZB}}$ and $\tau_{\text{rad SL}}$; 1.84, 1.809 and 1.799 eV for ME_W, ME_SL and ME_ZB, respectively, and 0.004–006 eV^{-1} for α. For the ZB-transitions the "background" decay time 1200 ps, corresponding to emission of longest (16 nm) sections and negative α values, describing decay increase, were used. Our $\tau(E)$ measurements allow assignment of two peaks observed in a single NW in spectra (Fig. 2 and 4) to W and ZB section emission. In NSOM spectra in Fig. 3 we can resolve a shoulder at 1.80 eV, which is related to SL transition.

Acknowledgements
Work was supported by the National Science Foundation via NSF-NIRT grant No. ECS-0609249.

References

[1] M. Kunol, *Phys. Chem. Chem. Phys.* **10**, 620 (2008).
[2] J. J. Gelennonet *et al*, *Phys. Rev. B* **80**, 0813303(R) (2009).
[3] F. Intoni *et al*, *Phys. Rev. B* **63**, 075313 (2001); A. Feltrin *et al*, *Phys. Rev. B* **69**, 205321 (2004).
[4] A. M. Mintairov *et al*, *Phys. Rev. B* **69** 15, 155306 (2004)
[5] A. M. Mintairov *et al*, *Phys. Stat. Sol. B* (in press) (2010).
[6] F. Dubin *et al*, *Nature Physics* **2**, 32 (2006).
[7] P. Jing *et al*, *J. Phys. Chem.* **113**, 13545 (2009).
[8] A. M. Mintairov *et alSemicond. Sci. Tech.* **24**, 075013 (2009).
[9] M. Queslati *et alPhys. Rev. B* **32**, 8220 (1985).